Dynamics About Uniformly Rotating Tri-Axial Ellipsoids. Application to Dynamics About Asteroids

D.J. Scheeres
Jet Propulsion Laboratory
California Institute of Technology
Pasadena, CA
E-Mail:djs@leelanau.jpl.nasa.gov

Abstract

The general problem of satellite and particle dynamics about a uniformly rotating tri-axial ellipsoid with constant density is formulated. The study of this problem can shed light on the dynamics of particles and satellites when orbiting irregularly shaped bodies such as asteroids. The physical specification of an asteroid modeled as a tri-axial ellipsoid can be reduced to two non-dimensional shape parameters (the eccentricities of the tri-axial ellipsoid) and one non-dimensional parameter which is a function of the body density, shape and rotation rate. All these parameters may be measured or inferred from ground-bad observations. Using these three parameters, the rotating ellipsoid may be classified into Type I or Type II ellipsoids depending on whether or not all synchronous orbits about the body are unstable. This classification of the ellipsoid has significant consequences for the dynamics of bodies in orbits which are near-synchronous with the asteroid rotation. Asteroids classified as Type I have stable motion associated with near-synchronous orbits. Asteroids classified as Type II have unstable motion associated with near-synchronous orbits. Families of planar periodic orbits are computed for two specific ellipsoids based on the asteroids Vesta and Eros. The stability of these families are computed and related to the type classification of the ellipsoid. Notes are also made on the existence of stable and unstable periodic orbits about the asteroid Ida. Analytic approximations are also introduced under some assumptions, leading to a simplified description of orbits about a tri-axial ellipsoid. Finally, a table of parameters and classifications for a few known asteroids and comets are given.

1 Introduction

In investigating particle and satellite orbits about irregularly shaped small Solar System bodies such as asteroids and comets, there are a variety of force perturbations which must be accounted for. These include the solar tide, solar radiation pressure, comet outgassing and perturbations due to gravitational harmonics. Solar tide perturbations dominate when fairly far from the body (see Hamilton and Burns, 1991). Radiation pressure forces generally cause small particles to crash on the asteroid surface, yet may not affect larger particles or artificial satellites to the same degree (see Hamilton and Burns, 1992). When close to the body the gravitational harmonics and, in the case of comets the outgassing presdominate the orbital dynamics. This paper concentrates on the effects of the non-spherical shape of the asteroid on orbits which are close to the body.

Traditional studies of satellite motion under gravitational perturbations have usually focused on the planetary case where these effects are relatively small compared to the attraction of the central body. When orbiting a small, non-spheroid body these classical analyses may no longer apply, due to the relatively large perturbations seen by orbiters. In studying orbiter dynamics about small bodies it is sometimes convenient to leave the gravitational harmonics formulation

aside and concentrate on specific mass distributions which have closed form solutions for their gravitational potentials. This allows the analyst to specify the major shape perturbations of the central body in closed form, rather than having to specify the many coefficients needed in a harmonic expansion of the gravity field. Some studies have taken advantage of this approach (Dobrovolskis and Burns, 1980; German and Friedlander, 1991; Chauvineau et al., 1993). In Dobrovolskis and Burns, 1980, the attraction of a tri-axial ellipsoid is used in conjunction with a number of other large perturbations to study ejecta in the special case of Phobos and bodies in similar situations. In German and Friedlander, 1991, some simple shapes (tri-axial ellipsoids, dual-spheres) are used to generate coefficients in a gravitational field expansion and the short term dynamics about such bodies are then investigated. In Chauvineau et al., 1993, the closed form gravitational potential of the tri-axial ellipsoid is used to search for chaotic orbits about a specific ellipsoid with a number of different rotation rates. Where comparable, agreement exists between their study and the current study.

Such an approach has also been used in the study of galactic dynamics (de Zeeuw and Merritt, 1983, Martinet and de Zeeuw, 1988, Merrill and de Zeeuw, 1983, Mulder and Hooimeyer, 1984). Generally, such studies use potentials with non-constant density distributions and concentrate on the dynamics of particles within the potential. Nonetheless, there are parallels between the study of dynamics outside of and inside of potentials, although the parameter spaces between the study of galactic dynamics and small body orbiters tend to differ. of specific interest in these studies are the existence of stable periodic orbits within the potential, as the existence of such orbits indicate possible paths stars may follow.

Should an actual shape of an asteroid be measured (Hudson and Ostro, 1994), it is possible to derive a harmonic expansion of the gravity field, assuming a constant density. Thus a closed form potential may be viewed as an idealization, lying between simple spherical models and actual harmonic expansions. The tri-axial ellipsoid model is significant, however, as it incorporates the effect of the major shape variations and can be specified based or I optical observations alone.

This paper presents a general formulation of orbiters about uniformly rotating tri-axial ellipsoids. It is seen that the physical problem may be specified by three non-dimensional parameters which may all be measured or inferred from ground-based observations. Lists of these parameters are given in the appendix for several asteroids. Then the dynamics of near-synchronous orbits about a general ellipsoid are studied. It is seen that there are two classes of rotating ellipsoids, one has 2 unstable synchronous orbits and 2 stable synchronous orbits (the planets fall into this type in general). The other class only has unstable synchronous orbits, which is a departure from the usual situation in solar system bodies and occurs for asteroids which tend to be more distorted, less massive or which spin faster. This class of ellipsoids have a strong instability associated with near-synchronous orbits. It is interesting to note that the asteroids Eros and Ida may be classified as such an ellipsoid. Next, families of direct and retrograde planar periodic orbits are computed about ellipsoids based on the asteroids Eros and Vesta. These asteroids are of different type, as discussed above, and the evolution of periodic orbit families about them are different. Notes on periodic orbits about the asteroid Ida are also given. Finally, some analytic approximations are introduced which explain some of the observed motion in terms of averaged osculating elements.

2 Model Specification and Derivation

The tri-axial ellipsoid model of a small body is specified once the size, shape, density and rotation rate of the small body is given. Various techniques for sire, shape and rotation rate determination from ground based observations are described in Magnusson et al., 1989. In depth explanations of these and other techniques can be found in *Asteroids II*, 1989, Section II. Improvements to the tri-axial ellipsoid shape are also possible (Ostro et al., 1990, Hudson and Ostro, 1994) but are not

considered here. Note that the density of an asteroid cannot be directly measured in most cases and must be inferred by comparison with known bodies (usually the minor planets, see Millis and Dunham, 1989).

Even with ground observations there is no specific information on the gravity field of the small body. The tri-axial ellipsoid provides a methodology for study which includes the major effects of the body's irregularity, as it incorporates the three major dimensions of the body into the force potential. Note that this model does not provide a general description of the gravity field of an asteroid, as it has three planes of symmetry. It is, however, a versatile model as it has a wide range of possible shapes generated by adjusting the shape parameters. Varying these, the body may be deformed from a sphere to a cigar to a pancake.

To specify the ellipsoid geometrically only the three major axes are needed. Given a constant density for the asteroid and its shape and size, there are classical formulae for the gravitational potential and its first and second partials. These formulae all entail evaluating elliptic integrals, for which simple and robust numerical procedures exist (Press et al., 1992, Section 6.11).

2.1 Physical Characteris ics

If the total size of a body is $a \times b \times c$, where $a \geq b \geq c$, then the associated tri-axial ellipsoid has major semi-axes of $a/2 \times b/2 \times c/2$. Let $\alpha = a/2$, $\beta = b/2$ and $\gamma = c/2$. Then the ellipsoid is specified by its major semi-axes $\alpha \times \beta \times \gamma$, where $\alpha \geq \beta \geq \gamma$.

Given a constant density ρ for the body, its gravitational parameter μ is computed as:

$$\mu = \frac{4\pi}{3} G\rho\alpha\beta\gamma \tag{1}$$

where G is the gravitational constant ($G = 6.672 \times 10^{-8}$ cm^{3}g^{-1}s^{-2}) and $\frac{4\pi}{3}\alpha\beta\gamma$ is the volume of the ellipsoid.

Define a body-fixed coordinate system in the ellipsoid. The $\hat{x}$ axis lies along the largest dimension α, the $\hat{y}$ axis lies along its intermediate dimension β and the $\hat{z}$ axis lies along its smallest dimension γ.

This analysis assumes that the ellipsoid rotates uniformly about its largest moment of inertia, thus the ellipsoid rotates uniformly about the $\hat{z}$ axis. The rotation rate of the ellipsoid is denoted as ω. It is possible to generalize this model to an ellipsoid with nutation and precession, but this is not performed in this analysis.

2.2 Gravitational Potential

The gravitational potential corresponding to a constant density tri-axial ellipsoid is classically known as a function of elliptic integrals. There are two forms of the potential, one if the point in question is in the interior of the ellipsoid and another if the point lies exterior to the ellipsoid.

If in the interior of the ellipsoid, the gravitational potential at a point $\hat{x}, \hat{y}, \hat{z}$ is (MacMillan, 1930, Sections 32-37):

$$V(\hat{x}, \hat{y}, \hat{z}) = \frac{3\mu}{4} \int_0^\infty \phi(\hat{x}, \hat{y}, \hat{z}; u) \frac{du}{\Delta(u)} \tag{2}$$

$$\phi(\hat{x}, \hat{y}, \hat{z}; u) = \left[\frac{\hat{x}^2}{\alpha^2 + u} + \frac{\hat{y}^2}{\beta^2 + u} + \frac{\hat{z}^2}{\gamma^2 + u} \right] \tag{3}$$

$$\Delta(u) = \sqrt{(\alpha^2 + u)(\beta^2 + u)(\gamma^2 + u)}. \tag{4}$$

Note that $V \leq 0$ always.

The generalization of this potential to the exterior of the ellipsoid is performed using Ivory's theorem. See MacMillan, 1930, Section 35 for a derivation of this result. Then the gravitational

potential of an ellipsoid at a point $\hat{x}, \hat{y}, \hat{z}$ exterior to the body is:

$$V(\hat{x}, \hat{y}, \hat{z}) = \frac{3\mu}{4} \int_{\lambda(\hat{x},\hat{y},\hat{z})}^{\infty} \phi(\hat{x}, \hat{y}, \hat{z}; u) \frac{du}{\Delta(u)} \tag{5}$$

$$\phi(\hat{x}, \hat{y}, \hat{z}; \lambda(\hat{x}, \hat{y}, \hat{z})) = 0 \tag{6}$$

where ϕ and Δ are defined as before. The parameter λ is a function of $\hat{x}, \hat{y}, \hat{z}$ and is solved for implicitly from equation (6) and defines the ellipsoid passing through the point $\hat{x}, \hat{y}, \hat{z}$ which is confocal to the body's ellipsoid. Equation (6) is a cubic equation in λ and has a unique positive root λ whenever

$$\phi(\hat{x}, \hat{y}, \hat{z}; 0) > 0 \tag{7}$$

(when $\hat{x}, \hat{y}, \hat{z}$ lies outside the ellipsoid), has the root $\lambda = 0$ when $\phi(\hat{x}, \hat{y}, \hat{z}; 0) = 0$ (when $\hat{x}, \hat{y}, \hat{z}$ lie on the ellipsoid surface), and is not needed in the interior of the ellipsoid (when $\phi(\hat{x}, \hat{y}, \hat{z}; 0) < 0$). Thus the potential defined by equations (5) and (6) is valid for the exterior and interior of the ellipsoid as long as $\lambda = 0$ whenever in the interior of the constant density ellipsoid.

To give the discussion clarity and generality, it is useful to normalize the variables via a time and length scale. Denote the scale time to be $1/\omega$ and the non-dimensional time as τ:

$$\tau = \omega t. \tag{8}$$

Choose the largest semi-axis of the ellipsoid, α, to be the length scale and the non-dimensional space variables to be x, y and z where

$$x = \hat{x}/\alpha \tag{9}$$

$$y = \hat{y}/\alpha \tag{10}$$

$$z = \hat{z}/\alpha. \tag{11}$$

2.3 Equations of Motion

The differential equations governing the motion of a point mass in a rotating coordinate frame is given as (Wintner, 1947, Chapter III):

$$\begin{aligned} \ddot{x} - 2\dot{y} &= U_x \\ \ddot{y} + 2\dot{x} &= U_y \\ \ddot{z} &= U_z \end{aligned} \tag{12}$$

where the potential U is defined as:

$$U = \frac{1}{2}(x^2 + y^2) - \delta V(x, y, z) \tag{13}$$

$$V = \frac{3}{4} \int_{\lambda}^{\infty} \phi(x, y, z; v) \frac{dv}{\Delta(v)} \tag{14}$$

$$\Delta(v) = \sqrt{(1+v)(\beta^2+v)(\gamma^2+v)} \tag{15}$$

$$\phi(x, y, z; v) = \frac{x^2}{1+v} + \frac{y^2}{\beta^2+v} + \frac{z^2}{\gamma^2+v} - 1 \tag{16}$$

$$\delta = \frac{\mu}{\omega^2 \alpha^3}. \tag{17}$$

The parameter $\lambda > 0$ is solved for from $\phi(x, y, z; \lambda) = 0$ whenever $\phi(x, y, z; 0) > 0$, else $\lambda = 0$. Also, the inequalities $1 \geq \beta \geq \gamma$ are assumed to hold. The notation U_x denotes the partial derivative of the potential U with respect to the variable x. Note that these equations are given in a rotating coordinate frame, which has an angular rate of unity in the normalized system of units adopted.

Any motion in these units is easily converted to dimensional units by applying the transformations (8) - (11).

The parameter δ is a function of the ellipsoid shape, size, density and rotation rate.

$$\delta = \frac{4\pi G\rho\beta\gamma}{3\omega^2} \tag{18}$$

Note that these are all quantities which may be inferred, to some degree of accuracy, from Earth based observations. The parameter δ is, effectively, the ratio of the gravitational acceleration to the centripetal acceleration acting on a particle at the longest end of the ellipsoid, assuming that the ellipsoid has all its mass concentrated at the origin. Should the ellipsoid be a sphere, then it is the true gravitational acceleration to centripetal acceleration ratio on the equator. See the appendix for a listing of this parameter for some known asteroids and comets. Note that the density of asteroids and comets is a poorly known quantity in general, thus we have assumed some nominal values in the following analysis (generally 3.5 g cm^{-3}).

2.4 Symmetries in the Equations of Motion

There are a number of symmetries present in these equations, due to the form of the potential U First note the three-fold symmetry of U:

$$U(x, y, z) = U(\pm x, \pm y, \pm z). \tag{19}$$

This holds as U and λ are functions of x^2, y^2 and z^2 only.

In terms of the full equations of motion, and the space and time coordinates, the equations are invariant under the transformations:

$$(x, y, z, \tau) \qquad x \; y, \quad z \; \tau \tag{20}$$

$$(x, y, z, \tau) \rightarrow (x, -y, z, -\tau) \tag{21}$$

$$(x, y, z, \tau) \rightarrow (-x \; y, z, -\tau) \tag{22}$$

These transformations may be composed onto each other to find additional invariant transformations.

Another way to view these transformations is as how they act on initial conditions and time. Motions starting from the following initial condition pairs can be transformed into each other under the appropriate transformations given above.

$$(x_o, y_o, z_o, \dot{x}_o, \dot{y}_o, \dot{z}_o, \tau_o) \rightarrow (x_o, y_o, -z_o, \dot{x}_o, \dot{y}_o, -\dot{z}_o, \tau_o) \tag{23}$$

$$(x_o, y_o, z_o, \dot{x}_o, \dot{y}_o, \dot{z}_o, \tau_o) \rightarrow (x_o, -y_o, z_o, -\dot{x}_o, \dot{y}_o, -\dot{z}_o, -\tau_o) \tag{24}$$

$$(x_o, y_o, z_o, \dot{x}_o, \dot{y}_o, \dot{z}_o, \tau_o) \rightarrow (-x_o, y_o, z_o, \dot{x}_o, -\dot{y}_o, -\dot{z}_o, -\tau_o) \tag{25}$$

The reversal of the time sign indicates that the transformed motion goes backwards in time.

A special subset of these initial conditions are those which transform into themselves, leading to motion which is symmetric about a line in a plane. Should any orbit have two such symmetries, then it is a periodic orbit (Marchal, 1990, Section 10.6). These are discussed later.

3 Jacobi Energy

There is an integral of motion immediatly apparent in the equations of motion (2). This results from the uniform rotation of the ellipsoid. The statement of this integral is:

$$T = \frac{1}{2}\left(\dot{x}^2 + \dot{y}^2 + \dot{z}^2\right) \tag{26}$$

$$T - U(x, y, z) = -C \tag{27}$$

where the parameter C is the Jacobi constant of the system, T is the kinetic energy of the satellite in the rotating coordinate frame and U is defined in equation 13. Given a set of initial conditions, the value of the resultant constant is conserved during all periods of motion. Note that the constant is conserved even if the particle trajectory intersects the ellipsoid in the course of its motion.

3.1 Zero-Velocity Surfaces

A brief description of the zero-velocity surfaces and their interpretation is given. This discussion has many similarities to the standard discussion of the zero-velocity surfaces in the restricted three-body problem (Moulton, 1914, Chapter VIII). Note that, by definition, $U > 0$. Thus if $C < 0$, then $T > 0$ and the satellite can never come to rest in the rotating frame. Further, then there are no *a priori* bounds on where the particle may not travel.

Conversely, should $C > 0$, then there is the possibility that $T = 0$ on some surface in x, y, space, called a surface of zero-velocity. These surfaces are important as they partition the space into regions of allowable ($T > 0$) and unallowable ($T < 0$) motion. Of special interest are any surfaces which guarantee that the particle is trapped in the vicinity of the ellipsoid or is bounded away from the ellipsoid.

As is the usual procedure in such analyses, first consider the zero-velocity surface when $C \gg 0$ and then discuss the changes in these surfaces as C decreases towards 0. Setting $T = 0$, the equation to solve to find the zero-velocity surfaces is:

$$\frac{1}{2}(x^2 + y^2) + \delta V(x, y, z) = C \tag{28}$$

Recall that $V(x, y, z) \leq 0$. Then note that $V(x, y, z) \geq V(0, 0, 0)$, thus if $C + \delta V(0, 0, 0) > 0$, there is only one solution to this equation, a perturbed cylinder of radius $r = \sqrt{2C + \delta V(x, y, z)} < \sqrt{2C}$. As $C \to \infty$, or as $z \to \pm\infty$, then $r \to \sqrt{2C}$. Motion is allowable outside of this cylinder only. As C decreases this cylinder moves inward.

When $C = -\delta V(0, 0, 0)$ another zero velocity surface bifurcates at the center of the ellipsoid. As C decreases further this zero-velocity surface expands and, depending on the parameters of the ellipsoid, will eventually intersect and then surround the ellipsoid itself, leaving space between the zero velocity surface and the surface of the ellipsoid. At this point, motion is allowable in the space above the surface of the ellipsoid, and such motion cannot escape from the vicinity of the ellipsoid. As before, there is still a zero-velocity surface which separates the space near the ellipsoid from the space far from the ellipsoid. Thus there is a band surrounding the ellipsoid where motion is not possible.

As the energy increases further, these two surfaces will touch at two symmetric points along the x-axis. The location of these points may be computed by solving the algebraic equation:

$$U_x(\pm x_o, 0, 0) = 0 \tag{29}$$

$$x_o \neq 0 \tag{30}$$

$$\lambda = x_o^2 - 1. \tag{31}$$

These points correspond to relative equilibrium points in the dynamical system and are called the saddle equilibrium points. The value of energy at these points is denoted by C_s. For C decreasing from C_s, particles may then travel between the space close to the ellipsoid and the space far from the ellipsoid.

As the energy decreases further, the zero-velocity surfaces projected in the x-y plane shrink to two symmetric points along the y axis, found by solving the algebraic equation:

$$U_y(0, \pm y_o, 0) = 0 \tag{32}$$

$$y_o \neq 0 \tag{33}$$

$$\lambda = y_o^2 - 1. \tag{34}$$

Again, these are equilib rium points and are called the center equilil rium points. The value of energy at these points is denoted by C_c. For decreasi ng C the zero-velocity surfaces th en do not intersect the x-y p lane and only exist in the out-of-plane space. As C - , 0^{+} , the zero-velocity surfaces shrink and n ove to the points $x = 0, y = 0, z = \pm\infty$, where they disappear when $C =$ ().

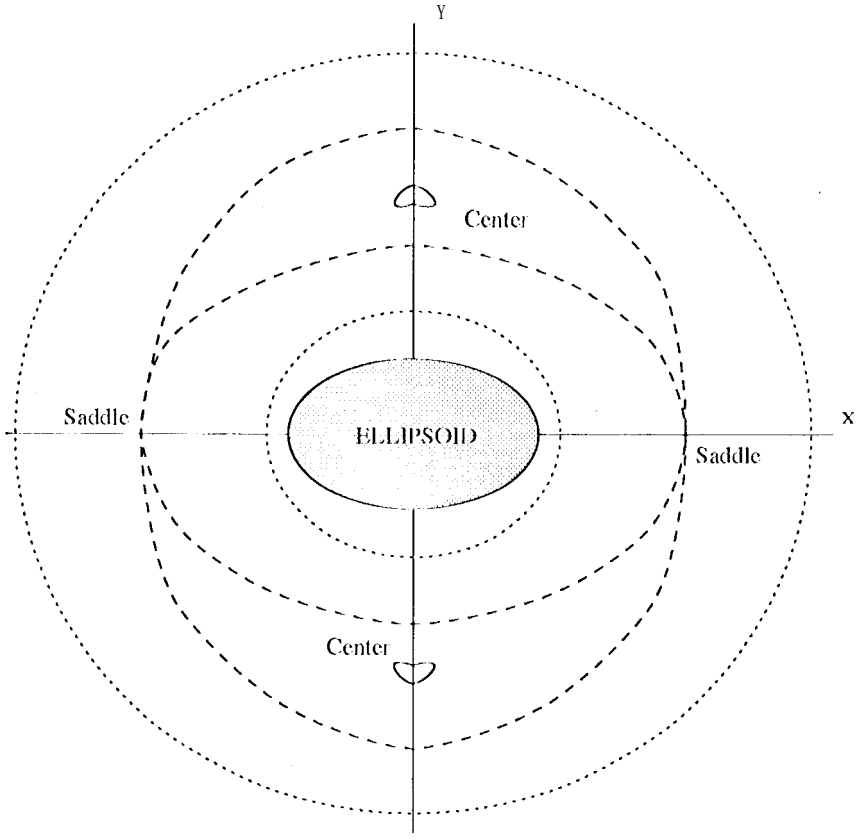

Figure 1: Zero-Velocity Curves for a Tri-Axial Ellipsoid

Note that these zero-velocity surfaces only have practical application when one considers direct orbits about the ellipsoid in inert ial space. Retrograde orbits (in inertial space) generally have T >>0 with respect the the rotating frame, and thus have C <0. Thus, while retrograde orbits often prove to be quite stable, their energy is such that there is no zero-velocity barrier between them and the ellipsoid. This points to deficiencies in using Hill stal bility as a complete characterization of stability of motion.

3.2 Hill-Stability Radius

A useful application of the energy integral is to determine the maximum radius at which a nominally circular orbit has an energy equal to or less than the value of energy at the saddle equilibrium points. Inside of this radius Hill stability may no longer exists and thus it is possible for the initially circular orbit to eventually crash onto the surface of the ellipsoid. outside of this radius Hill stability exists and provides a guarantee that the particle will never come within the zero velocity curves surrounding the ellipsoid. The energy value at the saddle equilibrium point

(with saddle equilibrium point location r_s) is:

$$C_s = \frac{1}{2}r_s^2 + \delta V(r_s, 0, 0) \tag{35}$$

The radius at which an initially circular orbit has an energy equal to the energy C_s, denoted as r^*, must be solved for from the equation:

$$C_s = \frac{1}{2}r^{*2} + \frac{1}{2}\left(\sqrt{\frac{\delta}{r^*}} - r^*\right)^2 + \delta V(0, r^*, 0) \tag{36}$$

This is a non-linear equation and must be solved for numerically. Note that the potential is evaluated along the y-axis as this gives the maximum radius at which an initially "circular)' orbit loses its Hill stability. Also note that the initial velocity is modified to be non-dimensional and is evaluated in the rotating coordinate frame. The value of r^* is given for some specific asteroid-like ellipsoids in the appendix.

4 Equilibrium Points and Their Stability

In studying direct orbits about an ellipsoid in an inertial frame, it is of interest to find circular, synchronous orbits. In the rotating reference frame, these synchronous orbits are equilibrium points of the equations of motion. For ellipsoids of revolution about the equator ($\alpha = \beta$), there are an infinity of such points. For a general tri-axial ellipsoid, there are at most four such points exterior to the body.

It is also of interest to compute the stability of these synchronous orbits. Classical results for orbits about planet-like ellipsoids reveal that two of these synchronous orbits are unstable and two are stable (cite). When investigating asteroid-or collIct-like ellipsoids, these results are not necessarily true. It then becomes possible for all four synchronous orbits to be unstable. This result has implications for satellite dynamics about an asteroid.

Algebraically, the equilibrium points are found by finding all solutions to the equations:

$$U_x(x_o, y_o, z_o) = 0 \tag{37}$$

$$U_y(x_o, y_o, z_o) = 0 \tag{38}$$

$$U_z(x_o, y_o, z_o) = 0. \tag{39}$$

From equation (13), $U_z = 0$ if and only if $z = 0$. Thus the problem may be reduced to finding all solutions of:

$$x_o\left[1 - \frac{3\delta}{2}\int_\lambda^\infty \frac{dv}{(1+v)\Delta(v)}\right] = 0 \tag{40}$$

$$y_o\left[1 - \frac{3\delta}{2}\int_\lambda^\infty \frac{dv}{(\beta^2+v)\Delta(v)}\right] = 0 \tag{41}$$

$$\phi(x_o, y_o, 0; \lambda) = 0. \tag{42}$$

Solutions to these equations are discussed in the following subsections. The solution $x = y = 0$, at the center of the ellipsoid, is not discussed.

The stability of these equilibrium points is also an item of interest, as the phase space surrounding these points may be characterized once their stability properties are known. The stability of motion in the vicinity of these points is inferred from a study of the solutions to the variational equations expanded about these points. Using such an analysis (Brouwer and Clemence, 1961, Chapter X), the conditions for the equilibrium points to be stable are:

$$U_{xx}|_o\, U_{yy}|_o > 0 \tag{43}$$

$$4 - U_{xx}|_o - U_{yy}|_o > 0 \tag{44}$$

$$(4 - U_{xx}|_o - U_{yy}|_o)^2 - 4U_{xx}|_o U_{yy}|_o > 0. \tag{45}$$

The out-of-plane oscillations about these equilibrium points are stable, as can be noted since the potential U is convex in the variable z about each point.

If all the stability conditions are satisfied, then the resulting motion is a harmonic oscillation about the equilibrium point. This oscillation has two fundamental frequencies associated with it. Each frequency describes a libration of the particle trajectory about the equilibrium point.

If stability condition (43) is violated, then condition (45) is satisfied and the resulting motion in the vicinity of the equilibrium point consists of a stable and unstable hyperbolic manifold and a harmonic oscillation. Should condition (44) be violated also, a similar result, applies.

If stability condition (45) is violated, then condition (43) is satisfied. Then the resulting motion in the vicinity of the equilibrium point consists of a stable and unstable spiral, i.e. consists of a hyperbolic motion multiplied by a rotation. In this case, all motion will in general spiral away from the equilibrium point.

Now the position and stability of each of the equilibrium points is investigated in turn.

4.1 Saddle Equilibrium Points

First consider the solution when $x_o \neq 0$ and $y_o = 0$. Note that x_o lies along the longest axis of the ellipsoid. The equation to solve in this case, reduces to:

$$1 = \frac{3\delta}{2} \int_{\lambda_o}^{\infty} \frac{dv}{(1+v)\Delta(v)} \tag{4(i)}$$

$$\lambda_o = x_o^2 - 1. \tag{47}$$

Note that the solution λ_o, and hence x_o also, may be expressed by a transcendental equation involving elliptic functions. We do not use this property explicitly, but instead solve equation (46), when necessary, using the implicit function theorem and Newton iteration. Call these the saddle equilibrium points, for reasons which will become obvious, and denote their coordinates by $\pm x_s$ and $y_s = 0$.

It is interesting to note that these equilibrium points are not guaranteed to exist. If the inequality

$$1 < \frac{3\delta}{2} \int_{0}^{\infty} \frac{dv}{(1+v)\Delta(v)} \tag{48}$$

is violated, then the saddle equilibrium points do not exist, either interior or exterior to the ellipsoid. Note the following inequality and identity,

$$1 = \frac{3}{2} \int_{0}^{\infty} \frac{dv}{(1+v)^{5/2}} \leq \frac{3}{2} \int_{0}^{\infty} \frac{dv}{(1+v)\Delta(v)} \tag{49}$$

This implies that a necessary condition for the inequality to be violated, and for the saddle points to not exist, is $\delta < 1$,

Should inequality (48) be violated, then it is imagined that the ellipsoid would not be physically stable as a particle placed at the end of the ellipsoid (at $x = \pm\alpha$) would fly off due to centripetal acceleration. Otherwise the body must have an internal cohesive force in addition to gravity.

To compute the stability of the saddle points, substitute the values x_s and y_s into the the second partial derivatives and simplify to find:

$$U_{xx}|_s = \frac{3\delta}{\Delta(\lambda_s)} \tag{50}$$

$$U_{yy}|_s = 1 - \frac{3\delta}{2} \int_{\lambda_s}^{\infty} \frac{du}{(\beta^2+u)\Delta(u)}. \tag{51}$$

Given that $\beta < 1$, then $U_{yy}|_s < 0$, as can be inferred from equation (46). It is also clear that $U_{xx}|_s > 0$. Thus stability condition (43) is clearly violated while condition (45) is satisfied. The status of condition (44) is not as clear. But, this stability condition does not change the basic instability type of the saddle points, which is hyperbolic. Thus, any satellite placed at or near these points will be influenced mostly by the hyperbolic stable and unstable manifolds, and its general motion will be to depart from the vicinity of the point. Also, it is possible to choose initial conditions in the neighborhood of the saddle points to find periodic orbits (albeit unstable). Note that the saddle equilibrium points are similar to the L_1, L_2 and L_3 equilibrium points in the restricted three-body problem (Moulton, 1914, Chapter VIII).

As seen in Section 3, the saddle points are the boundary points between regions of allowable motion close to and far from the ellipsoid. Thus, motion starting close to these points will in general either be trapped near the ellipsoid or trapped away from the ellipsoid. Another way of stating this is to note that one pair of each of the point's stable and unstable manifolds lies close to the ellipsoid while the other pair lies away from the ellipsoid. Thus, when passing close to these points in phase space, the final motion of a satellite will be close to or far from the ellipsoid depending upon which pair of manifolds the satellite is influenced by.

4.2 Center Equilibrium Points

Next consider the solution for $x_o = 0$ and $y_o \neq 0$. Recall that the y_o axis lies along the intermediate size length of the ellipsoid. The equations to solve for this case reduce to :

$$1 = \frac{3\delta}{2} \int_{\lambda_o}^{\infty} \frac{du}{(\beta^2 + u)\,\Delta(u)} \tag{5'2}$$

$$\lambda_o = y_o^2 - \beta^2 \tag{53}$$

Again, the solution for λ_o and y_o may be expressed by a transcendental equation involving elliptic functions. Call these equilibrium points the center equilibrium points. Their coordinates are denoted as $x_c = 0$ and $\pm y_c$. They are important for characterizing the asteroid with respect to satellite motion.

Similar to the saddle points, there are cases when these equilibrium points do not exist. A necessary condition for these points to not exist is that the saddle points not exist. We assume in general that these equilibrium points exist in the ellipsoids under consideration.

To compute the stability of these points, substitute the values x_c and y_c into the the second partial derivatives and simplify to find:

$$U_{xx}|_c = 1 - \frac{3\delta}{2} \int_{\lambda_c}^{\infty} \frac{du}{(1+u)\Delta(u)} \tag{54}$$

$$U_{yy}|_c = \frac{3\delta}{\Delta(\lambda_c)}. \tag{55}$$

Given that $\beta < 1$, then $U_{xx}|_c > 0$, as inferred from equation (52). It is also clear that $U_{yy}|_c > 0$. Thus stability condition *(43)* is clearly satisfied. The status of conditions (44) and (45) are not as clear, and may or may not be satisfied, depending on the parameters of the ellipsoid: δ, β, γ.

A few notes may be made concerning the order in which conditions (44) and (45) may be violated. Assume that the parameter δ is fixed and that the parameters β and γ will be decreased from 1 $\beta = \gamma = 1$ (keeping $\gamma \leq \beta$), thus deforming a sphere into an ellipsoid. Taking equations (54) and (55) to the limit for a sphere yields

$$\lim_{\beta,\gamma \to 1} U_{xx}|_c = 0 \tag{56}$$

$$\lim_{\beta,\gamma \to 1} U_{yy}|_c = 3 \tag{57}$$

Under these limits, both condition *(44)* and *(45)* are satisfied. Given this, and that condition *(43)* is satisfied, it is evident that condition (45) must be violated before condition *(44)* may be violated when deforming a sphere into a general ellipsoid. Thus, as a body is progressively deformed from a sphere, it is stability condition *(45)* that delineates between whether the center points are stable or unstable. If condition *(44)* becomes violated subsequently, it will not have as large a qualitative effect as it will only pertain to the orientation of the stable and unstable manifolds of the center points and will not affect the instability type.

For ellipsoids where all the stability conditions are satisfied, the center points are stable in the sense that motions started near them will oscillate about the center point indefinitely. For ellipsoids where the stability condition is not satisfied, the center points become complex unstable. Then, any motion started near the center point will spiral away from or towards the center point. As there are 110 isolating zero- vclocit,y surfaces associated with the center points, the final motion will be to either fall onto the ellipsoid or escape from the ellipsoid.

Whether the center points are stable or unstable has a large influence on the stability of near-synchronous orbits about the ellipsoid. When the center points are stable, motion started in near synchronous orbits tend to remain bounded away from the ellipsoid, as the region of regular curves in phase space near the center points makes passage through these curves to the surface of the ellipsoid difficult. It is noted in passing that near-circular orbits about ellipsoids with stable center points seem to be well behaved in general, with any instabilities acting in longitude only.

The same cannot be said when the center points are unstable. Now the phase space around the center points is influenced by the unstable spiral manifolds. The generic motion under the influence of these manifolds is to spiral away from the center point. It is important to note that the spiral the satellite will follow tends 10 act in both the angular and radial directions. The generic motion of a satellite along these unstable manifolds seems to either crash into the ellipsoid or to suffer repeated close approaches to it. Due to the distorted shape of the ellipsoid, these close approaches may cause the satellite to gain hyperbolic speeds and escape the ellipsoid. If the motion is continued through crashes with the ellipsoid the generic final motion associated with the unstable manifold is a departure from the vicinity of the ellipsoid. Thus, near-synchronous orbits about ellipsoids with unstable center points can be characterized as being unstable in general. It is not uncommon to observe a near-synchronous, near circular orbit crash onto an ellipsoid (with unstable center points) within a matter of days,

In this paper ellipsoids with stable center equilibrium points are called Type] ellipsoids, while those with unstable center equilibrium points are called Type II ellipsoids. It is evident that the crashing problem associated with Type 11 ellipsoids is related to near synchronous motion about the ellipsoid. Thus, when orbiting about a Type II ellipsoid, it is in general best to avoid near synchronous orbits. Conversely, it will be unlikely to find orbiting debris in near-synchronous orbits about Type 11 ellipsoids.

5 Computing Ellipsoid Type

It is of interest to characterize when an ellipsoid is of Type 1 (stable center points) and when it is of Type II (unstable center points). In general, this characterization is a function of the three parameters: β, γ, δ. Given these numbers for any ellipsoid, it is possible to compute stability condition (45) and check which category the ellipsoid falls into. This condition may be represented as a two-dimensional surface in the three-dimensional space β, γ, δ. Figure (2) presents a projection of this surface onto the $\beta \times \delta$ plane for values of $\gamma =$ (), $\beta/2, \beta$. Given specific values of β, γ and δ, the ellipsoid is of Type II if it lies beneath the appropriate curve in figure (2). Finally observe that the curves do not extend all the way to $\beta =$ 1, For $\gamma = \beta$, the curve stops at a value of $\beta \approx$ ().928. For $\gamma < \beta$ the curve stops at an increasing value. In general, for all β greater than these values at the end of the curve, the ellipsoid can only be of Type 1. This is intuitively evident

as any oblate ellipsoid (,/? = 1) is definitely of Type 1 independent of γ, and hence there will in general be a small interval less than $\beta = 1$ where the Type 1 property is maintained.

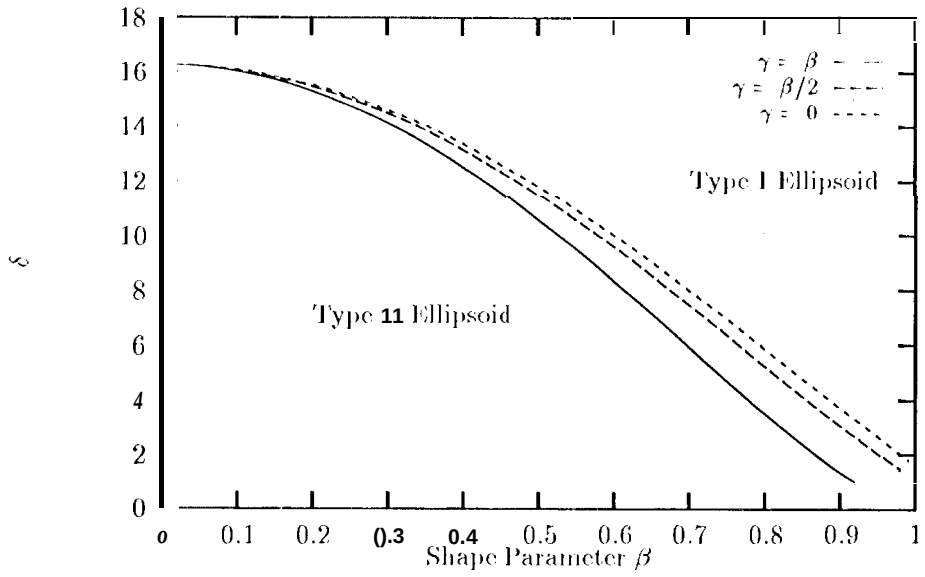

Figure 2: δ for a Type I ellipsoid vs β (for $\gamma = 0 \to \beta$)

Note that a sufficient condition for an ellipsoid with parameters β, γ and δ to be of Type II is that the corresponding ellipsoid with $\gamma = \beta$, with δ held constant, be of Type II, This result is apparent from figure (2). This sufficiency condition simplifies the computation as the two dimensional surface in the three dimensional space is now collapsed into a one dimensional surface (a line) in the two dimensional space β, δ. The ellipsoid is, in this case, an ellipsoid of revolution. It is a prolate ellipsoid with its axis of rotation perpendicular to the axis of symmetry, similar to a cigar lying on a table with its rotation axis perpendicular to the table. There are simplifications to the form of the stability condition for this case,

First note the following results for the center equilibrium point, assuming that $\gamma = \beta < 1$. These results are computed using the properties of the elliptic integrals.

$$U_{xx}|_c = 3\left(1 - \frac{\delta}{\Delta(\lambda_c)}\right) \tag{58}$$

$$U_{yy}|_c = -\frac{3\delta}{\Delta(\lambda_c)} \tag{59}$$

$$\Delta(u) = (\beta^2 + u)\sqrt{1 + u} \tag{60}$$

Additionally, it is now possible to reduce the elliptic integrals to quadratures in terms of known functions. The equation from which we solve for λ_c is still, however, transcendental.

The condition for stability (equation (45)) now reduces to:

$$1 > -\frac{36\delta}{\Delta(\lambda_c)}\left(1 - \frac{\delta}{\Delta(\lambda_c)}\right) \tag{61}$$

sill).jcct to the constraint

$$1 = \frac{3\delta}{2}\left[\frac{\sqrt{1+\lambda_c}}{(1-\beta^2)(\beta^2+\lambda_c)} - \frac{1}{2(1-\beta^2)^{3/2}}\ln\left\{\frac{1+\sqrt{\frac{1-\beta^2}{1+\lambda_c}}}{1-\sqrt{\frac{1-\beta^2}{1+\lambda_c}}}\right\}\right| \tag{62}$$

Note that δ is a function of μ, α and ω^2. Thus δ will decrease if the mass (or density) of the ellipsoid decreases or if the size or rotation rate increases. These effects tend to make a Type I ellipsoid into a Type II ellipsoid.

In a previous paper (Chauvineau et al., 1993), orbits were investigated about a body with normalized shape parameters $\alpha = 1, \beta = 1/\sqrt{2}, \gamma = 1/2$ and with a variety of δ parameters, $\delta =$ 129.76, 32.44,8,11,2.03 corresponding to rotation periods of 40, 20, 10 and 5 hours. Note that these parameters are defined using our notation. The density of the body was assumed to be 2.5 gcm^{-3}. As stated in that paper, the ellipsoid with rotation rates of 40, 20 and 10 hours has stable center equilibrium points and thus are Type I ellipsoids as discussed here. When the rotation period is 5 hours, however, the center equilibrium points are unstable and thus the ellipsoid is a Type 11 ellipsoid. From our current analysis, this indicates a qualitative difference between the longer period ellipsoids and the shorter period (5 hour) ellipsoid. The difference being that the shorter period ellipsoid will have severe instability in the vicinity of the synchronous orbits, as was noted in Chauvineau et al., 1993. It is expected that the longer period ellipsoids will have regions of (radially) stable motion associated with near-synchronous orbits. Due to differences in parameter space, the analysis carried out in that paper does not apply directly to the results discussed here, as that paper concentrated more on slowly rotating asteroids.

6 Periodic Orbits

Now our discussion] focuses on a few families of periodic orbits computed for satellite motion about an ellipsoid. These results are all numerical and are computed for only a few specific ellipsoid shapes and parameters. Two classes of planar periodic orbits are discussed, one direct and the other retrograde with respect to inertial space. Both these families degenerate into circular orbits as $\beta, \gamma \to 1$. In computing the periodic orbits, the families are either terminated once an intersection with the ellipsoid occurs or when the continued computation of the family becomes too difficult.

These orbits all lie in the ellipsoid equatorial plane ($z \equiv 0$). The near-circular direct and retrograde orbits have two distinct symmetries, and thus have a quarter-symmetry in the plane (similar to Hill's Variation orbit, Wintner, 1947, Chapter VI). The following pairs of boundary conditions are used to compute these orbits:

$$\begin{aligned} x(t_0) &= x_0 \\ y(t_0) &= 0 \\ \dot{x}(t_0) &= 0 \\ \dot{y}(t_0) &= \dot{y}_0 \end{aligned} \tag{63}$$

$$\begin{aligned} x(t_1) &= 0 \\ y(t_1) &= y_1 \\ \dot{x}(t_1) &= \dot{x}_1 \\ \dot{y}(t_1) &= 0 \end{aligned} \tag{64}$$

Should any orbit satisfy both of these boundary conditions, then that orbit may be extended into a periodic orbit symmetric about both the x and y axes. In the following numerical studies we choose two basic ellipsoids to investigate, one based on the asteroid Vesta, which may be classified as a Type I asteroid, and the other based on the asteroid Eros, which may be classified as a Type II asteroid, Notes are also added on periodic orbits about the ellipsoid based on the asteroid Ida, which may also be classified as a Type II asteroid.

The stability computations of the periodic orbits follow well established procedures for planar periodic orbits (Hénon, 1965). The actual method used is described in Scheeres, 1992,

Sections 6.9.2-6.9.4. They involve computation of a characteristic quantity a which must satisfy the condition $|a| < 1$ for the orbit to be stable. A similar quantity may be computed which describes the out-of-plane stability of the orbit. Files containing the initial conditions for the periodic orbits are available by request from the author.

6.1 Vesta

Vesta may be classified as a Type 1 ellipsoid. See the appendix for a list of the physical properties of the asteroid Vesta. Thus, there are two stable equilibrium points and two unstable equilibrium points surrounding it. The following computations are given in normalized units. The lengths are converted to kilometers via multiplication by 265. The unstable saddle equilibrium points are located at:

$$x_s = \pm 1.94097 \tag{65}$$

$$C_s = 5.565129 \tag{66}$$

The stable center equilibrium points are located at:

$$y_c = \pm 1.92377 \tag{67}$$

$$C_c = 5.531994 \tag{68}$$

The minimum circular orbit radius to ensure Hill stability against crashing onto the ellipsoid is $r^* = 2.26$ in normalized units.

There are two families of periodic orbits associated with each center equilibrium point. Analogous to the periodic orbits associated with the triangle equilibrium points in the restricted 3-body problem (Moulton, ***1914,*** Chapter VIII), these two families may be distinguished as a long period family and a short period family. There is also a family of unstable periodic orbits associated with each saddle equilibrium point. This family is related to the one harmonic frequency about the equilibrium point in the linear approximation.

The family of retrograde periodic orbits is stable for all x_o. Note that the family of direct orbits at Vesta is stable over most of its range, except for some small regions of marginal stability or small instability. This strengthens the assertions of the previous section regarding Type 1 ellipsoids, as it is clearly possible for a satellite to follow a stable, direct orbit with altitudes close to the ellipsoid surface.

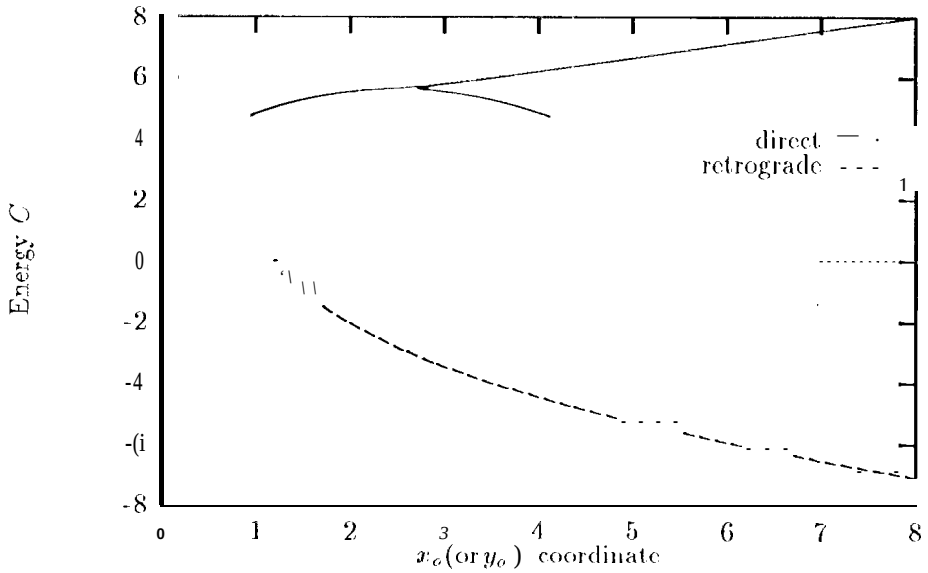

Figure 3: Periodic Orbit Families About Vesta

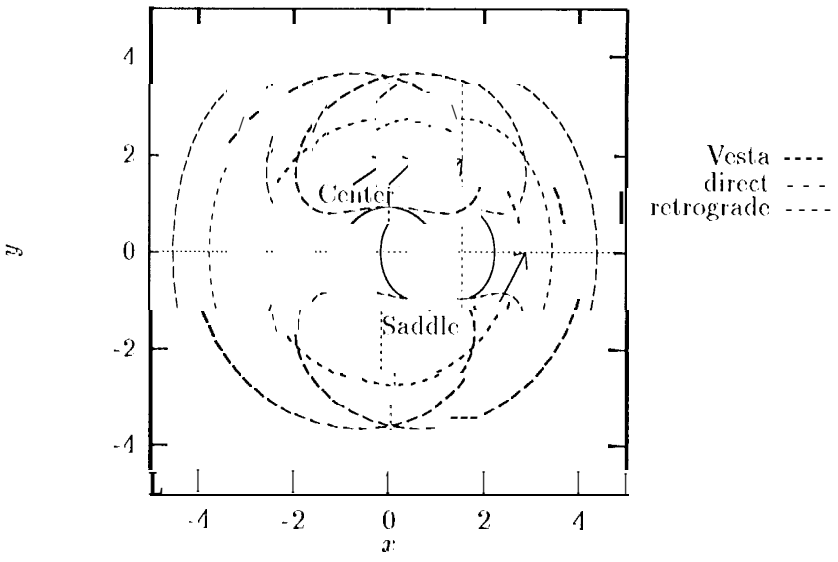

Figure 4: Sample Periodic Orbits About Vesta

Figure (3) shows the periodic orbit families as lines in the x_o, y_o, C space, where x_o is the initial coordinate along the x-axis, y_o is the coordinate along the y-axis where the orbit crosses perpendicularly and C is the energy of the orbit Note that the direct orbit splits from an essentially circular orbit into an orbit with a definite periapsis and apoapsis. The periapsis of the orbit lies along the y-axis, and crosses this axis perpendicularly. Conversely, the apoapsis lies along the x-axis and crosses this axis perpendicularly.

From the information on the plot the periodic orbit may be constructed as follows: given x_o, y_o : 0 and C, $\dot{y}_o$ may be computed by assuming that $\dot{x}_o$ = 0. This completely specifies the initial conditions for the orbit.

Figure (4) shows samples of a direct and retrograde periodic orbit. Note that both of the periodic orbits in this plot are stable. Also shown are two of the equilibrium points. Note that the saddle and center orbits and points have associated mirror images located 011 the other side of the asteroid, not shown in the figure,

6.2 Eros

The ellipsoid based on the asteroid Eros is a Type 11 ellipsoid. A Type Hellipsoid has four unstable equilibrium points in a uniformly rotating reference frame. The parameters used for the ellipsoid based on Eros are listed in the appendix. Note that, for convenience, the density was chosen so that δ = 1. Normalized units are used for the following computations. The lengths are converted to kilometers via multiplication by 20. The saddle equilibrium points are located at:

$$x_s = \pm 1.1926 \tag{69}$$

$$C_s = 1.6965 \tag{70}$$

The center equilibrium points are located at:

$$y_c = 40.92680 \tag{71}$$

$$C_c = 1,4'2333 \tag{72}$$

The minimum circular orbit radius to ensure Hill stability is r^* = 2.17 in normalized units. For these bodies the center points no longer generate periodic orbits in their vicinity. This is due to the local nature of the phase space about these equilibrium points, as closed orbits cannot be constructed in the linear system close to the unstable center points.

The presentation of the direct and retrograde periodic orbit families for the ellipsoid based on Eros are shown in figure (5). The definitions and interpretations of these orbits remains as before. There are some differences for these families, however. Most importantly, note that the direct orbits become unstable at a distance of 1.85 normalized units from the long end of the ellipsoid (at a radius of 37 km), and remains so for the remainder of the family, except for the small regions where the family curve passes through an extremum with respect to the energy C. This falls within the hill stability radius of 2.17 normalized units, implying that the unstable manifold of the orbit may intersect the ellipsoid, which it dots in general. Conversely, as might be expected, the retrograde orbits are stable throughout the family, even though these orbits never have the hill stability. Thus retrograde orbits may be considered "[safe" orbits in which to fly close to such an asteroid. Note the similar conclusion arrival at in Chauvineau, et al., 1993.

Not obvious in figure (5) is that the line defining the direct family of periodic orbits in figure (5) terminates as a spiral in the (x_o, C) plane and dots not intersect the ellipsoid. The stability parameter of this family becomes arbitrarily large as the family is continued along this curve.

In figure (6) are some samples of periodic orbits about the ellipsoid based on Eros. In this plot the direct orbit is unstable while the retrograde orbit is stable.

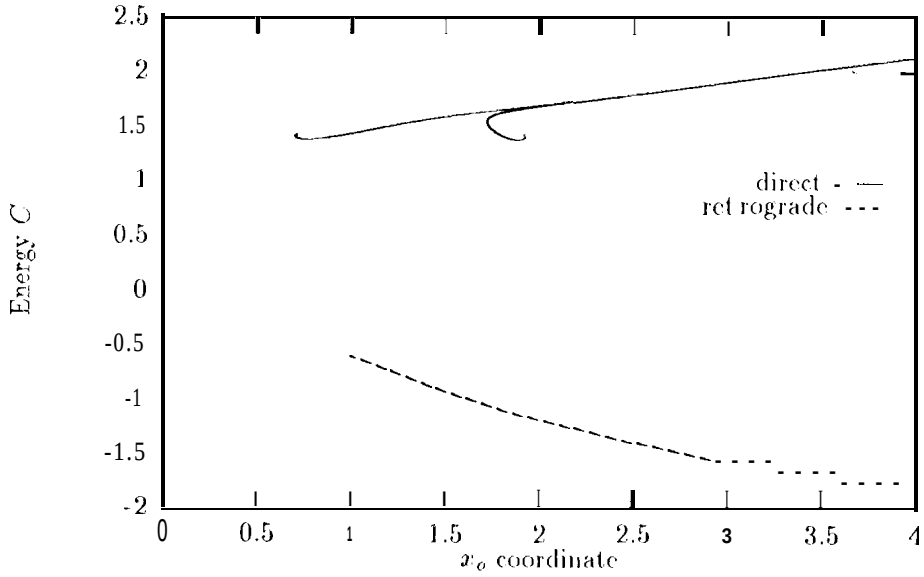

Figure 5: Periodic Orbit Families About Eros

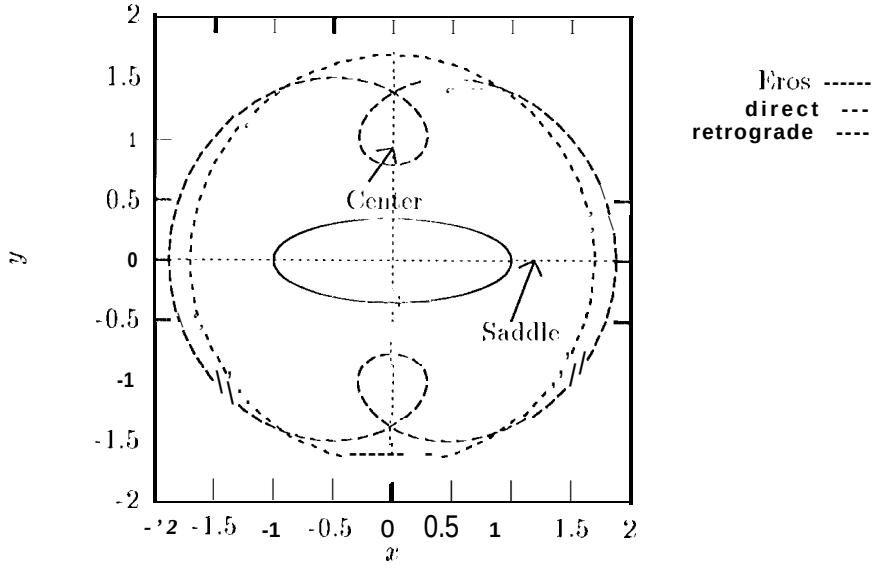

Figure 6: Sample Periodic Orbits About Eros

6.3 Ida

The ellipsoid based on the asteroid Ida is a Type II ellipsoid. Again a Type II ellipsoid has four unstable equilibrium points in a uniformly rotating reference frame. The parameters Used for the ellipsoid based on Ida are listed in the appendix. The density was assumed to be 3.5 gcm^{-3}. The normalized units are used for the following computations. The lengths are converted to kilometers via multiplication by 28. The unstable saddle equilibrium points are located at:

$$x_s = \pm 1.2105 \tag{73}$$

$$C_{is} = 1.7899 \tag{74}$$

The unstable center equilibrium points are located at:

$$y_c = \pm 0.9719 \tag{75}$$

$$C_c = 1.5366 \tag{76}$$

The minimum circular orbit radius to ensure Hill stability is $r^* = 2.14$ in normalized units ($= 59.9$ km). This establishes the possibility of stable, near circular orbits outside of 61 km. Note that a satellite of Ida has been discovered recently (Marsden, 1994). The estimated distance of the satellite from Ida is 100 km.

The direct and retrograde periodic orbits may also be computed for this ellipsoid. They are qualitatively similar to the families presented for Eros. Note that for Ida the direct doubly-symmetric periodic orbits are stable for all x_o greater 1.90 units (53.1 km). Inside of this limit, these orbits become unstable in general. As for Eros, the retrograde doubly-symmetric periodic orbits are stable for all x_o.

7 Non-Synchronous Motion

Finally some simple results are discussed which apply to satellite motion when not close to low-order resonances (namely not at a low altitude and not close to a 1:1 resonance with the asteroid rotation rate). This situation occurs when the satellite is far from the ellipsoid or is in a retrograde orbit about the ellipsoid. In the first case the ellipsoid will rotate beneath the spacecraft with a relatively large frequency, thus only high-order resonances will exist, and their strength will be muted by the larger radius. In the second case, the satellite travels in the opposite sense of the ellipsoid rotation, destroying resonances in general. In both situations the effects of the equatorial ellipticity in the gravitational potential tend to average to zero. This leaves the terms of zero order as the most significant gravitational effects on the satellite. This, in turn, is equivalent to the satellite being subject to a the field of an oblate spheroid. There is a wealth of classical results pertaining to orbits about an oblate spheroid. See Brouwer, 1959, Garfinkel, 1958 and Kozai, 1959 for some of the seminal work performed on this problem.

7.1 Major Effects of an Oblate Spheroid Model

The primary perturbation relating to an oblate spheroid model are the gravitational harmonic coefficients of degree 2 and 4 and Of order 0, C_{20} and C_{40}. Given a constant density tri-axial ellipsoid, these parameters may be computed as (German and Friedlander, 1991 ; note the missing factor of 2 in the denominator of their expression for C_{40}):

$$C_{20} = -\frac{1}{10\alpha^2}\left(\alpha^2 + \beta^2 - 2\gamma^2\right) \tag{77}$$

$$C_{40} = -\frac{3}{280\alpha^4}\left[3\left(\alpha^4 + \beta^4\right) + 8\gamma^4 + 2\alpha^2\beta^2 - 8\left(\alpha^2 + \beta^2\right)\gamma^2\right. \tag{78}$$

The major effect of these terms is the presence of secular motions in the node and argument of periapsis of the satellite orbit. Expressions for these secular rates can be found in Kozai, 1959; equations (27) and (28). The remaining elements are constant, on average, although all elements suffer short period variations with attendent non-zero means.

These results predict the stability results found for the direct periodic orbits far from the ellipsoid and for the retrograde periodic orbits about the ellipsoid. Further, comparisons between analytic formulae (Kozai, 1959) and numerical integrations of satellite orbits about an ellipsoid show overall qualitative agreement, should the proper assumptions apply.

7.2 Comparison between Numerical and Analytical Computation

In Plots (7) - (9), nodal regression rates for circular orbits at Eros, Vesta and Ida are presented. Each plot compares numerically computed secular nodal rates about the asteroids (modelled using the appropriate tri-axial ellipsoid) with analyticly derived secular nodal rates using Kozai's theory incorporating the C_{20} and C_{40} gravitational coefficientagain corresponding to the appropriate tri-axial ellipsoids. See Brouwer, 1959, for a definition of Kozai's gravity coefficients. The numerical computation was performed by integrating the appropriate orbit about the tri-axial ellipsoid for 1 day and computing the precession of the orbit angular momentum vector over that period.

Note the good agreement between analytical and numerical results for all retrograde orbits (i > 90). The orbits at Eros and Ida (a = 50 km, e = 0 and a = 100 km, e = 0 respectively) both show good agreement throughout the entire inclination range. This is a function of the orbits being far enough from the body for the averaging effects to exist. Note the poor agreement in the Vesta case for near-polar and direct orbits. This is due to a resonance between the orbit and Vesta's rotation rate. The period of a 500 × 500 km orbit at Vesta is ≈5.2 hours, while the rotation period of Vesta is assumed to be 5.3 hours. Thus, the presence of resonance invalidates the applicability of the analytical formulae, as is obvious from figure (8). Note that for the results to be applicable, the orbits must be stable in semi-major axis, eccentricity and inclination. All orbits plotted below satisfy this stability.

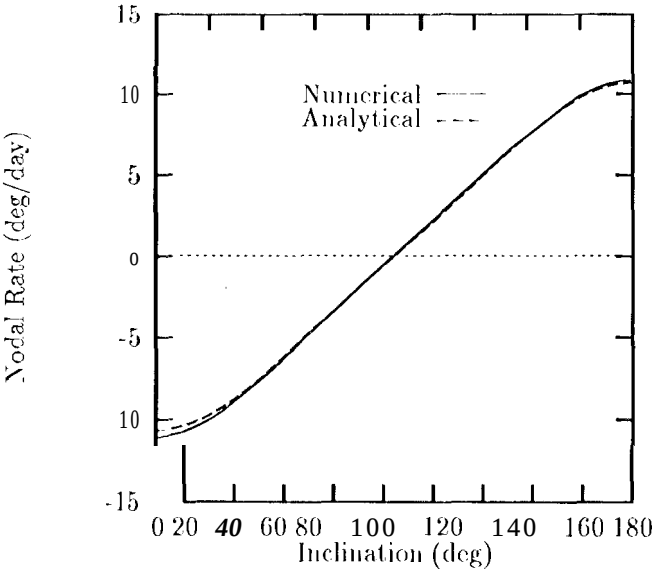

Figure 7: Secular Node rates at Eros for a = 50 km, **c** = 0

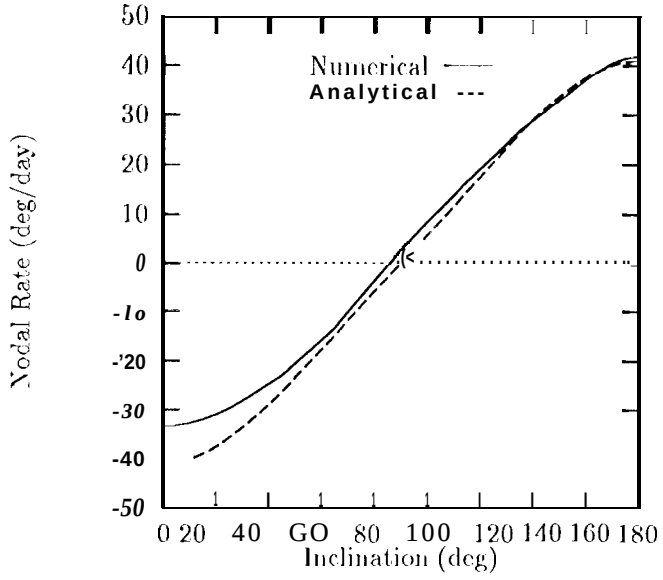

Figure 8: Secular Node rates at Vesta for $a = 500$ km, $e = 0$

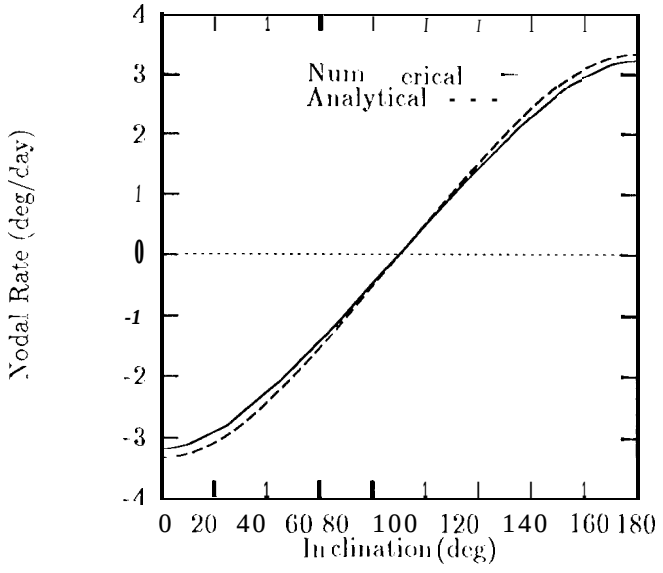

Figure 9: Secular Node rates at Ida for $a = 100$ km, $e = 0$

8 Conclusion

The research described in this paper defines the problem of satellite and particle dynamics about a tri-axial ellipsoid and arrives at some elementary results for this problem. All necessary formulae needed to compute the forces for a satellite orbiting a tri-axial ellipsoid have been presented. The problem has been non-dimensionalized and shown to depend on only three non-dimensional parameters; two shape parameters and one parameter relating the mass, size and rotation rate of the ellipsoid. Values of these parameters may be inferred from ground based measurements.

The zero-velocity surfaces of a satellite in orbit about the ellipsoid have been defined and described. The application of Hill stability to circular orbits was also discussed, in the context of a guarantee against collision with the ellipsoid. All synchronous circular orbits about the ellipsoid are found as well as the conditions for their existence. The stability of these synchronous circular orbits is discussed and two classes of ellipsoids are defined according to whether any of the synchronous orbits are stable or not. Some specific computations of periodic orbit families for two representative ellipsoids, based on the asteroids Vesta and Eros, are presented. Additionally, notes on stable and unstable orbits about the asteroid Ida tire made.

An important item discussed in this paper is the existence of two types of uniformly rotating ellipsoids, called herein as Type I and Type II ellipsoids. Near-synchronous orbits about a Type I ellipsoid tend to be stable and well behaved in a global sense. Conversely, near-synchronous orbits about a Type II ellipsoid tend to be unstable and usually crash onto the ellipsoid over very short time spans (on the order of days).

The distinction between Type I and Type II ellipsoids was also highlighted by the stability of the direct periodic orbit family about the Vesta based ellipsoid and the instability of the direct periodic orbit family about the Eros based ellipsoid. Note that in both cases the retrograde periodic orbit families were stable.

Finally, comparison between simple analytic results for oblate spheroids are compared with numerical results. Good agreement can be found if the orbiter is in a retrograde orbit or if the orbit is sufficiently distant from the asteroid.

Appendix

Following are tables (1) and (2) giving the physical and computed parameters of a few asteroids and a comet. The values of these parameters are approximate and are not necessarily based on the best available data.

Table (1) lists the basic physical dimensions and quantities associated with each body. Note that all of these quantities may be measured or inferred from ground-based observations. Table (2) contains the derived quantities stated in this paper. These include the Type of the ellipsoid (1 or II), the defining non-dimensional parameters β, γ and δ, the location of the saddle equilibrium point (x_s), the location of the center equilibrium point (y_c) and the maximum radius at which initially circular orbits are not Hill stable (r^*). All lengths in this table are in normalized units. The last two ellipsoids, called Mean 1 and Mean2, were taken from Chauvineau et al., 1993 and are representative of the ellipsoid studied in that paper.

Name	α (km)	β (km)	γ (km)	$2\pi/\omega$ (hours)	Density (g/cm^3)	C_{20} (-)	C_{40} (-)
Vesta	265	250	220	5.3	3.5	.051	.006
Ida	28	12	10.5	4.63	3.5	.090	.025
Eros	20	7	7	5.27	3.2	.088	.025
Gaspra	9.5	6	5.5	7	3.5	.072	.015
Tempel 2	8	4.25	4.25	8.9	1.0	.072	.017
Mean 1	$\sqrt{2}l$	l	$l/\sqrt{2}$	10	2.5	.100	.024
Mean 2	$\sqrt{2}l$	l	$l/\sqrt{2}$	5	2.5	.100	.024

Table 1: Physical parameters for some select small bodies

Name	$\hat{\beta}$	γ	δ	Type	Saddle	Center	r^*
Vesta	0.94	0.83	7.06	I	1.04	1.92	2.26
Ida	0.43	0.37	1.11	II	1.21	0.97	2.14
Eros	0.35	0.35	1.00	II	1.19	0.93	2.17
Gaspra	0.63	0.58	5.75	II	1.86	1.76	2.57
Tempel 2	0.53	0.53	2.07	II	1.39	1.22	2.19
Mean 1	$1/\sqrt{2}$	1/2	8.11	I	2.07	2.00	2.73
Mean 2	$1/\sqrt{2}$	1/2	2.03	II	1.37	1.25	2.08

Table 2: Derived quantities for some select small bodies

Acknowledgments

The author thanks J.K. Miller, N.X. Vinh, B.G. Williams and D.K. Yeomans for their comments, information and encouragement. The research described in this paper was carried out by the Jet Propulsion Laboratory, California Institute of Technology, under contract with the National Aeronautics and Space Administration.

References

Binzel, R.P., T. Gehrels & M.S. Matthews Eds, 1989. *Asteroids II*, University of Arizona Press

Brouwer, D., 1959. Solution of the Problem of Artificial Satellite Theory Without Drag, *The Astronomical Journal*, **64**, 378 - 397.

Chauvineau, B., P. Farinella & F. Mignard, 1993. Planar Orbits about a Triaxial Body: Application to Asteroidal Satellites, *Icarus*, **105**, 370 - 384.

de Zeeuw, T., D. Merritt, 1983. Stellar Orbits in a Triaxial Galaxy. I. Orbits in the Plane of Rotation, *The Astrophysical Journal*, **267**, 571 - 595.

Dobrovolskis, A.R., J.A. Burns, 1980. Life near the Roche Limit: Behavior of Ejecta from Satellites Close to Planets, *Icarus*, **42**, 422 - 441.

Garfinkel, B., 1958. On the Motion of a Satellite of an Oblate Planet, *The Astronomical Journal*, **63**, 88 - 96.

German, D., A. Friedlander, 1991. A Simulation of Orbits Around Asteroids Using Potential Field Modeling. *Proc. AAS/AIAA Spaceflight Mechanics Meeting*, Houston, TX February 11-13, 1991

Hamilton, D.P., J.A. Burns, 1991. Orbital Stability Zones about Asteroids, *Icarus*, **92**, 118 - 131.

Hamilton, D.P., J.A. Burns, 1992. Orbital Stability Zones about Asteroids II: The Destabilizing Effects of Eccentric Orbits and of Solar Radiation, *Icarus*, **96**, 43 - 64

enon, M., 1965. Exploration Numerique du Probleme Restreint. II., *Annales D'Astrophysique*, **28**, 992-1007.

Hudson, R.S., S.J. Ostro, 1994. Shape of Asteroid 4769 Castalia (989 PB) from nversion of Radar Images. *Science*, **263**, 940 - 943.

Kozai, Y., 1959. The Motion of a Close Earth Satellite, *The Astronomical Journal*, **64**, 367 - 377.

MacMillan, W.D., 1930. *The Theory of the Potential*, McGraw-Hill.

Magnusson, P. et al., 1989. Determination of Pole Orientations and Shapes of Asteroids. In *Asteroids II* (R.P. Binzel, T. Gehrels & M.S. Matthews, Eds.), pp 66-97, University of Arizona

Marchal, C., 1990. *The Three-Body Problem*, Elsevier.

Marsden, B.G., International Astronomical Union, Circular No. 5948, March 12, 1994.

Martinet, L., T. de Zeeuw, 1988. Orbital Stability in Rotating Triaxial Stellar Systems, *Astronomy and Astrophysics*, **206**, 269 - 278.

Merritt, D., T. de Zeeuw, 1983. Orbital Configurations for Gas in Elliptical Galaxies, *The Astrophysical Journal*, **267**, L19 - L23.

Millis, R.L., and D.W. Dunham, 1989. Precise Measurement of Asteroid Sizes and Shapes from Occultations. In *Asteroids II* (R.P. Binzel, T. Gehrels & M.S. Matthews, Eds.), pp 148 - 170, University of Arizona Press.

Moulton, F.R., 1914. *An Introduction to Celestial Mechanics, 2nd Edition*, MacMillan.

Mulder, W.A., J.R.A. Hooimeyer, 1984. Periodic Orbits in a Rotating Triaxial Potential, *Astronomy and Astrophysics*, **134**, 158 - 170.

Ostro, S.J., K.D. Rosema & R.F. Jurgens, 1990. The Shape of Eros, *Icarus*, **84**, 334 - 351.

Press, W.H., S.A. Teukolsky, W.T. Vetterling and B.P. Flannery, 1992.

Numerical Recipes in Fortran, 2nd Ed., Cambridge University Press.
Scheeres, D.J., 1992. *On Symmetric Central Configurations with Application to Satellite Motion About Rings*, Doctoral Dissertation, The University of Michigan.
Wintner, A., 1947. *The Analytical Foundations of Celestial Mechanics*, Princeton University Press.